

# THERMAL HARDENING AND STRUCTURE OF A PHOSPHORUS CONTAINING CEMENTITIOUS MODEL MATERIAL Phosphoric acid–wollastonite

G. Mosselmans<sup>1</sup>, Monique Biesemans<sup>2</sup>, R. Willem<sup>2</sup>, J. Wastiels<sup>1</sup>, M. Leermakers<sup>3</sup>, H. Rahier<sup>4\*</sup>, S. Brughmans<sup>4</sup> and B. Van Mele<sup>4</sup>

<sup>1</sup>Department of Mechanics of Materials and Constructions, Vrije Universiteit Brussel, Pleinlaan 2, Brussels, Belgium

<sup>2</sup>Department of Polymer Science and Structural Chemistry (High Resolution NMR Centre), Vrije Universiteit Brussel Pleinlaan 2, Brussels, Belgium

<sup>3</sup>Department of Analytical and Environmental Chemistry, Vrije Universiteit Brussel, Pleinlaan 2 Brussels, Belgium

<sup>4</sup>Department of Polymer Science and Structural Chemistry (Physical Chemistry and Polymer Science), Vrije Universiteit Brussel, Pleinlaan 2, Brussels, Belgium

The reaction of phosphoric acid with wollastonite has been studied for reaction mixtures with a molar ratio  $r=P/Ca$  from 0.39 up to 2.9. X-ray diffraction (XRD) and Fourier transform infrared spectroscopy (FTIR) reveal the formation of the crystalline products brushite (when  $r$  is smaller than 1.4) and monetite and calcium dihydrogenphosphate monohydrate (when  $r$  is above 1). Magic angle spinning nuclear magnetic resonance spectroscopy (MAS NMR) and FTIR show that amorphous silica is also formed which contains some residual calcium and hydroxyl groups. The proposed reactions are confirmed by the evolution of the reaction enthalpy measured with differential scanning calorimetry (DSC). The reaction was monitored with temperature modulated DSC (TMDSC) and dynamic mechanical analysis (DMA). The sharp increase of the elasticity modulus coincides with the onset of decrease in heat capacity. The setting of the reaction mixture does not slow down the reaction rate.

**Keywords:** material science, MTDSC, phosphorous, wollastonite

## Introduction

Rapidly setting cements enjoy great industrial interest. The fast setting of these materials is for example important for dental cements [1–3], rapid road repair [4, 5] and natural bone cements [6]. As a benefit of their fast setting, phosphate cements [4, 5, 7–9] can provide an appropriate solution. Magnesium phosphates [4, 5, 10–12], zinc phosphates [3, 9], aluminum phosphates [1, 3] and calcium phosphates [1, 2, 6, 7] can be distinguished. These phosphate materials are made by mixing a liquid and a solid phase. For some powder mixtures, water can be used as the liquid phase [4]. By addition of accelerators and/or retarders, the setting time can be adjusted [10]. In contrast with ordinary cements (e.g. Portland cement), these phosphate cements solidify in acid rather than in alkaline environment.

In this paper, the reaction of a phosphoric acid solution with a calcium source is investigated as a model, for a construction material developed at the university. Many calcium sources (like calcium carbonate and calcium hydroxide) react too fast with a phosphoric acid solution. The high heat production

and reaction rate result in materials with bad mechanical properties. To overcome this problem, sources that release calcium more slowly have to be used, such as sintered materials or more stable minerals. In this work, wollastonite ( $CaSiO_3$ ) will be used.

The products, obtained by the reaction of a phosphoric acid solution with wollastonite, are characterized in this work by a combination of magic angle spinning nuclear magnetic resonance spectroscopy (MAS NMR), Fourier transform infrared spectroscopy (FTIR) and X-ray diffraction (XRD). Preliminary experiments on reaction kinetics are obtained by using dynamic mechanical analysis (DMA), and (temperature modulated) differential scanning calorimetry, (TMDSC) [13, 14].

## Experimental

### Materials

A 13 mol% ortho-phosphoric acid solution was used, obtained by dilution with demineralised water of 51 mol% ortho-phosphoric acid from Merck. Wollastonite ( $CaSiO_3$ ) NYAD<sup>®</sup>200 of NYCO was

\* Author for correspondence: hrahier@vub.ac.be

used. The wollastonite contains about 4 mass% of impurities (like diopside and garnet). These impurities were taken into account to calculate the molar ratio  $r=P/Ca$  of the phosphoric acid–wollastonite mixture. To obtain a homogeneous and representative wollastonite, three bags (25 kg) of NYAD<sup>®</sup>200 were mixed, using a concrete mixer. The sample was divided into one kilogram portions and stored in plastic bags in hermetically closed containers.

The samples used for the spectroscopic techniques were obtained by mixing the appropriate amount of phosphoric acid and wollastonite, followed by keeping this mixture in a closed mould (thickness 2 mm) at 25°C for at least one day. Temperature has been measured and did not increase more than 3°C during this reaction.

In order to study the reaction, about 4 g of sample was mixed with a mechanical stirrer during 2 min while cooled in an ice bath to minimize the reaction conversion before the sample was brought into the analyser. At the start of the reaction, the pH of the mixture is about 0. Therefore, for all calorimetric measurements, gold coated stainless steel high-pressure sample pans (Mettler) were used to avoid reaction between sample and pan. Samples of molar ratios  $r=P/Ca$  above 1.33 were mixed in the pan to avoid sedimentation prior to sampling. About 25 mg of sample was used for each experiment.

The concentration of soluble P and Ca after reaction were obtained by crushing the material, adding demineralised water (30 mL to 1 g of sample), shaking the mixture intensively for 1 min (by hand) and performing a vacuum filtration on the suspension during 2 min using a water pump. On the filtrates, elemental analyses (P and Ca) were performed to determine the concentrations of soluble P and Ca left in the mixture after reaction.

## Methods

### TMDSC

TMDSC measurements were performed on a DSC822<sup>°</sup> Mettler with HSS7 cell, mechanical cooling and ADSC option. The purge gas was N<sub>2</sub> (50 mL min<sup>-1</sup>). The uncertainty margin on the reaction enthalpies is about 5% [14].

For TMDSC-experiments, heat capacity was calibrated with water. A temperature modulation of 0.5°C per 200 sec was applied for all experiments. Non-isothermal experiments were performed at a heating rate of 5°C min<sup>-1</sup>.

### DMA

A DMA7 instrument from PerkinElmer was used with a stainless steel parallel plate probe (diameter 1 mm).

To monitor the setting isothermally with DMA, the fresh reaction mixture was poured into a cylindrical container, covered with a thin rubber seal. On the seal a static load of 100 mN and a dynamic load of 90 mN were applied. Helium was used as a purge gas with a flow of 50 mL min<sup>-1</sup> [14].

### MAS NMR

<sup>29</sup>Si and <sup>31</sup>P MAS NMR spectra were obtained on a Bruker Avance 250 spectrometer, operating at 49.70 and 101.25 MHz for the <sup>29</sup>Si and <sup>31</sup>P resonance frequencies, respectively. For solid-state experiments rotors of 4 mm diameter and a spinning rate of 10 kHz were used. Typically, <sup>29</sup>Si spectra were obtained over a spectral width of 9.9 kHz (acquisition time: 0.2 s), with 1000 scans and a relaxation delay of 5 s. It was checked that this time was long enough for full relaxation. The <sup>31</sup>P spectra were acquired over a spectral width of 20 kHz (acquisition time: 0.1 s), with 200 scans and a relaxation delay of 5 s. The <sup>29</sup>Si spectra were deconvoluted with the software PERCH [15], in order to obtain the relative amounts of the different types of Si moieties. The chemical shift values of MAS NMR signals were calculated by taking the maxima of the individual resonances obtained from the spectral deconvolutions.

### FTIR

FTIR spectra were obtained with a FTIR PerkinElmer 1720X using KBr pellets. For pellet preparation, 1 mg of sample and 300 mg KBr were mixed and ground in a Wig-L-Bug for 5 min. A pellet of 200 mg from this mixture was made for analysis.

### XRD

XRD diffractograms of powdered samples of wollastonite and reaction products are registered on a Siemens D5000 diffractometer, generating a CuK<sub>α</sub> radiation with an applied voltage of 40 kV and a current of 40 mA.

### Elemental analysis

Analysis of Ca and P were performed using inductively coupled plasma atomic emission spectrometry (ICP-AES) (Thermo Jarell Ash Iris Advantage). The instrument was equipped with a concentric nebuliser, cyclonic spraychamber and radial plasma. Ar was used as carrier gas.

Calibration was performed using multielement standards prepared from single element standards (Johnson Matthey). To correct for instrumental drift and matrix effects an internal standard (Au: 25 ppm,

Y: 15 ppm) was used. The internal standard was introduced together with the sample in the nebuliser. Selected wavelengths for the analyses are 318.1 nm for Ca and 214.9 nm for P. The limits of quantification for Ca and P are  $10 \mu\text{g L}^{-1}$ .

## Results and discussion

### The phosphoric acid–wollastonite reaction

As mentioned in the introduction, phosphate cements are known to be fast reacting systems. The heat-flow signal, measured by quasi-isothermal TMDSC (Fig. 1), reveals that at  $25^\circ\text{C}$  the reaction is almost complete after 200 min (for  $r$  equals 0.69). The heat flow signal of Fig. 2, which is proportional to the reaction rate, visualizes that at the start of the reaction, the reaction rate is not at maximum. After a partial heat conversion of 25%, a sharp increase in reaction rate is observed. This indicates either the consumption of an inhibitor or the autocatalytic nature of the reaction.

After the first local maximum, a second maximum in heat flow is observed. The complex shape of the exotherm can be caused by a combination of different successive reaction steps and/or by the specific heterogeneous reaction conditions. Further investigation is needed.

In a non-isothermal DSC experiment, performed after this isothermal reaction, no further exothermic reaction is observed. This is an indication that full-conversion can be reached under isothermal conditions even though the material solidifies. The reaction enthalpies of the isothermal experiments are calculated by integration of the heat flow signal. For the example shown in Fig. 2, the reaction enthalpy is  $-226 \text{ J g}^{-1}$  ( $-89 \text{ kJ mol}^{-1} \text{ P}$ ;  $-62 \text{ kJ mol}^{-1} \text{ Ca}$ ).

Figure 2 also shows the evolution of the storage modulus (DMA) during the reaction. One must take into account that the experimental set-up influences

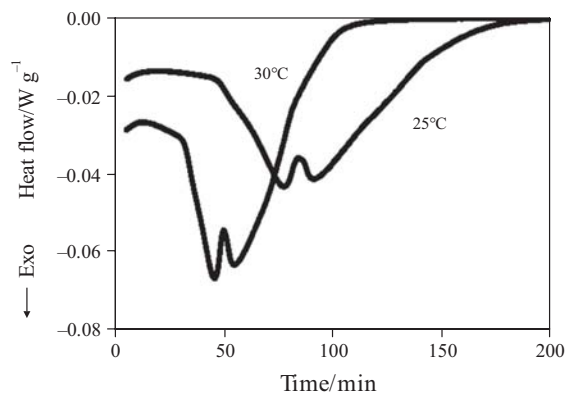


**Fig. 1** Isothermal reaction of a mixture with  $r=0.69$ . The heat flow signals (obtained by MTDSC) are shown for isothermal reaction at 25 and  $30^\circ\text{C}$

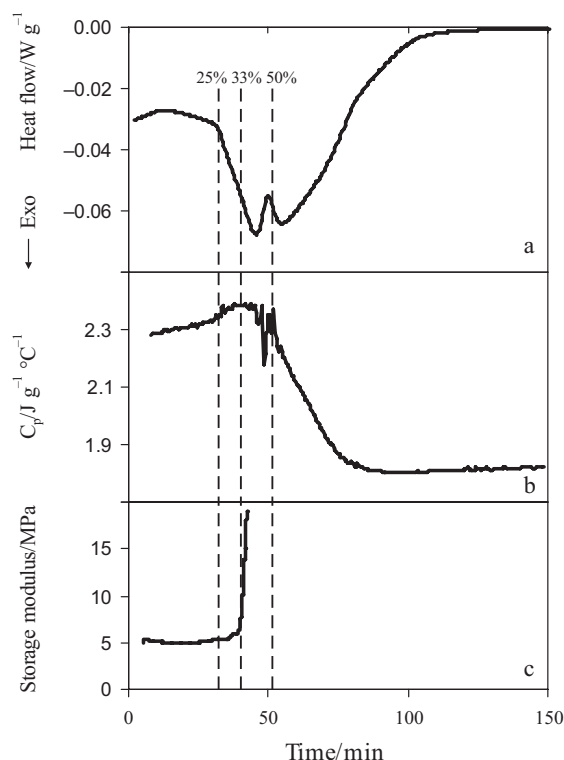


**Fig. 2** Isothermal reaction of a reaction mixture with  $r=0.69$  at  $30^\circ\text{C}$ . a – Heat flow and b –  $C_p$  signal (both obtained by TMDSC) are shown together with c – storage modulus (obtained by DMA). The vertical dotted lines indicate the times at which the heat conversion reaches 25, 33 and 50% of the total heat conversion indicating the onsets of the increase in reaction rate, the increase in storage modulus and the decrease of the  $C_p$ -signal, respectively

the value of the storage modulus. Nevertheless, the time at which the storage modulus suddenly increases can be assigned to the beginning of the setting of the material. By comparing this signal to the heat-flow signal one can conclude that setting sets in after only 33% of heat conversion, while the heat-flow signal is still increasing. Thus, the solidification process does not influence the reaction rate at first sight. The same behaviour is observed for other inorganic low-temperature curing materials [14, 16]. As mentioned above, for the phosphoric acid–wollastonite reaction, full-conversion is reached during isothermal reaction at low temperature.

An important benefit of DSC is the possibility to measure the heat capacity ( $C_p$ ) during quasi-isothermal experiments. For the experiments in this work, it may be assumed that no excess contributions are involved [17]. The evolution of  $C_p$  during the phosphoric acid–wollastonite reaction is depicted in Fig. 2. At the start of the reaction, the heat capacity increases due to the formation of intermediates and/or end-products with a higher  $C_p$  value than the initial components. Preliminary experiments show the appearance of  $\text{Ca}^{2+}$  in the

**Table 1** XRD peaks (intensity in arbitrary counts at a specific value of  $2\theta$ ) of the different crystalline components after reaction at 25°C for mixtures with molar mixing ratio  $r$  in the range  $r=0.42$  up to  $r=1.66$ . Small peaks with an intensity in the order of magnitude of the noise are excluded

$r$	Brushite	Calcium dihydrogenphosphate monohydrate	Monetite	Wollastonite
	$2\theta=11.7^\circ$	$2\theta=18.1^\circ$	$2\theta=24.1^\circ$	$2\theta=26.8^\circ$
0.55	537	–	–	388
0.69	638	–	–	127
0.83	736	–	–	61
0.97	902	–	40	–
1.11	412	65	136	–
1.39	–	101	277	–
1.66	–	173	511	–

liquid phase extracted from wollastonite as will be elaborated elsewhere [18]. It is known that  $\text{Ca}^{2+}$  forms several soluble products in phosphoric acid solution [19] that may be responsible for the increase in  $C_p$ . At 33% of heat conversion, i.e. the start of setting as seen by DMA, the  $C_p$  signal levels off. At a higher conversion (about 50%) the  $C_p$ -signal decreases stepwise to a value lower than the initial  $C_p$ . This drop in  $C_p$  is due to the transformation of a viscous reaction suspension into a solid material. It is remarkable that the heat capacity signal gets constant before the heat flow signal returns to the baseline. In many other systems the inverse is observed [14].

### Reaction stoichiometry and product characterisation

#### XRD

The molecular structure of the reaction products was investigated with a combination of techniques. XRD-analyses of reacted samples with different molar ratios are summarized in Table 1. Literature search points out that, for  $r < 1$ , brushite ( $\text{CaHPO}_4 \cdot 2\text{H}_2\text{O}$ ) and residual wollastonite are the only crystalline components present in the material. The amount of residual wollastonite decreases when  $r$  tends to 1, while the opposite is true for brushite.

For  $1 < r < 1.66$  (highest value measured), three crystalline products are observed: brushite, monetite ( $\text{CaHPO}_4$ ), and calcium dihydrogenphosphate monohydrate ( $\text{Ca}(\text{H}_2\text{PO}_4)_2 \cdot \text{H}_2\text{O}$ ). The amount of brushite becomes smaller when  $r > 1$ , and vanishes between  $r=1.2$  and 1.4. No crystalline silicon containing reaction products are observed with XRD for  $r > 1$ .

#### MAS NMR

The  $^{29}\text{Si}$  MAS NMR spectrum for a mixture with  $r=0.69$  is shown in Fig. 3. The width of the signals is typical for amorphous materials. Three different chemical environments can be discriminated for the Si atoms in this sample, at  $-112$ ,  $-102$  and  $-88$  ppm. The resonance at

$-88$  ppm is attributed to crystalline wollastonite ( $\text{Q}^2$ ).  $\text{Q}^n$  denotes a  $\text{SiO}_4$  tetrahedron connected to  $n$  other  $\text{SiO}_4$  tetrahedra [20, 21]. The presence of wollastonite and the amorphous nature of the Si containing reaction products are in accordance with the results obtained by XRD. The rather broad resonance for the crystalline wollastonite as received (width at half height 300 Hz) points out that the material is rather disordered. The resonance at  $-112$  ppm is attributed to amorphous silica ( $\text{Q}^4$ ). The resonance at  $-102$  ppm is attributed to an amorphous  $\text{Q}^3$  type silicon. The network modifier can be either calcium or hydrogen as will be explained further on. The first step in the reaction with the phosphoric acid is probably the extraction of Ca without a complete disruption of the wollastonite grains [18]. This was concluded from preliminary elemental analysis results on the liquid fraction showing Ca in solution whereas the dimensions and the shape of the wollastonite grains do not change. Wollastonite will reorganize during this process through exchange of  $\text{Ca}^{2+}$  for  $2\text{H}^+$  ions and formation of more Si–O–Si bridges (higher degree of cross-linking). This explains the presence of  $\text{Q}^3$  and  $\text{Q}^4$  type silicon atoms. As a result the order in the crystalline structure is disturbed resulting in peak broadening (width of  $\text{Q}^3$  and  $\text{Q}^4$  is 300 and 385 Hz, respectively).

The overlap of the broad resonances makes deconvolution of the signals necessary to obtain a reliable quantification of the different Si surroundings (Fig. 3). The inset in Fig. 3 shows  $^{29}\text{Si}$  MAS NMR spectra of mixtures with different  $r$  values. One can see that the signal assigned to residual wollastonite decreases when  $r$  increases to 1. The amount of  $\text{Q}^3$  and  $\text{Q}^4$  Si atoms is about 25 and 75%, respectively, of the reacted wollastonite for  $r < 1$ . For molar ratios of 1 or higher, no residual wollastonite can be found, in agreement with XRD data, even though a broad resonance occurring at  $-94$  ppm arises, probably from another type of amorphous  $\text{Q}^2$  Si environment formed during the reaction (width of this  $\text{Q}^2$  is 470 Hz). This signal represents about 5% of the Si groups. However, it is possible that this

new  $Q^2$  is also present for  $r < 1$ , causing an over-estimation of the amount of residual wollastonite. The amount of  $Q^3$  and  $Q^4$  Si atoms for  $r > 1$  is about 40 and 55%, respectively. The counter-cation for these  $Q^2$  and  $Q^3$  configurations can be  $H^+$  or residual  $Ca^{2+}$ . Ca is used to form brushite in the ratio of one Ca atom for one P atom. For  $r > 1$  there will be no residual  $Ca^{2+}$  thus  $H^+$  is the only counter-cation possible. The amount of  $Q^2$  and  $Q^3$  Si atoms formed, when compared to the total amount of reacted Si, is approximately 25% for  $r$  up to 1. For  $r > 1$ , this amount is raised to 45%. If the contribution of Ca is negligible, this means that the same amounts of the  $SiO_4$  tetrahedra (i.e. 45% if  $r > 1$ ) bear one or two OH groups.

With  $^{31}P$  MAS NMR (not shown), only reso-

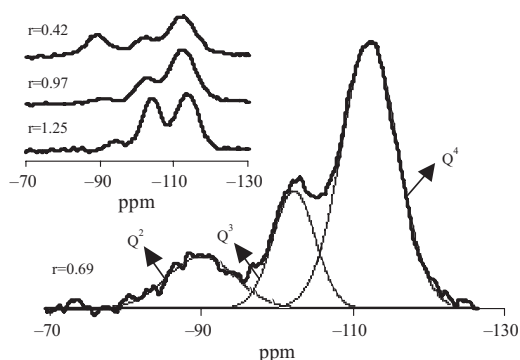


**Fig. 3**  $^{29}Si$  MAS NMR spectrum of a sample with  $r=0.69$  reacted at  $25^\circ C$ . The thin lines show the result of deconvolution of the spectrum. In the inset, spectra for different mixing ratios ( $r=0.42, 0.97$  and  $1.26$ ) are displayed

nances around 0 ppm are observed (+3.2, +1.5 and  $-0.2$  ppm), corresponding to monophosphates [9, 12]. Upon increasing the molar ratio  $r$ , the resonance at 1.5 ppm becomes more important at the expense of the other ones. For  $r > 0.83$  it is the only important signal.  $^{31}P$  NMR-spectroscopy does not appear particularly useful to characterise these phosphorus-containing products. The sharpness of the signals indicates that these monophosphates are crystalline, in agreement with the XRD-measurements.

### FTIR

For  $r > 1$ , the FTIR spectra reveal the presence of amorphous silica, brushite and calcium dihydrogenphosphate monohydrate, in agreement with the XRD-measurements (Fig. 4). Due to the similarity of the spectra of brushite and monetite, monetite cannot be detected in the presence of brushite. For the sake of clearness the spectrum of amorphous silica has been subtracted in Fig. 4.

The FTIR spectra of reacted samples with different molar ratios  $r < 1$ , (not shown) prove that the specific absorptions of wollastonite (for example at 903,

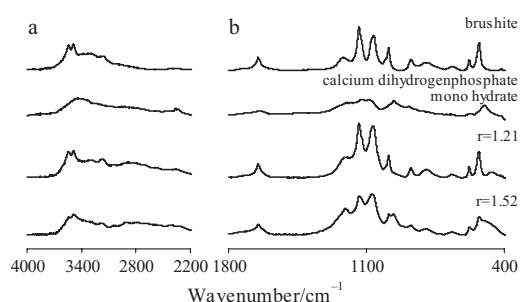


**Fig. 4** FTIR-spectra of the reaction products brushite and calcium dihydrogenphosphate monohydrate and of the reaction mixture  $r=1.21$  and  $1.52$  reacted at  $25^\circ C$

929 and  $966\text{ cm}^{-1}$ ) decrease as  $r$  increases. At molar ratio  $r=0.93$  no specific wollastonite absorptions can be noticed any more. One can conclude that for  $r < 1$ , brushite and amorphous silica are clearly present and traces of wollastonite can be found. This is in line with the findings from XRD and NMR.

### DSC

As mentioned before, the reaction enthalpy can be calculated from isothermal DSC experiments. Conventional DSC experiments were performed for different molar ratios.

Figure 5 shows the reaction enthalpies per mol of Ca and P. Different reaction regimes appear [22]. If a sub-stoichiometric quantity of phosphoric acid is used (this means a value of  $r < 1$ ), all the phosphoric acid will be able to react. Thus, the reaction heat/mol P must be constant as long as all the phosphoric acid will react. There is a large scatter on the data caused by the difficulty to obtain a homogeneous mixture of solid with a small amount of liquid and to take a sample representative for the whole mixture. The solid horizontal line in Fig. 5a is the mean value of the reaction enthalpies measured up to  $r=1$ , and is  $-88\text{ kJ/mol P}$ . This constancy is valid only if phosphorus is consumed in the formation of one single product, which is the case for molar ratios below 1, as previously proven by XRD, NMR and FTIR. For Ca, the reaction enthalpy per mol Ca should increase linearly with  $r$  (line Fig. 5b), as is clearly the case up to  $r=1$ . For mixtures with  $r > 1$  the reaction enthalpy/mol Ca is observed to be constant and equal to  $-88\text{ kJ/mol Ca}$ . This was not expected because of the different reaction products formed simultaneously but in variable ratios, depending on  $r$ . This constant value implies that for the formation of the different products, the reaction enthalpy per mol Ca is comparable. If more phosphoric acid is used, the amount of phosphoric acid present in excess will reduce the reaction enthalpy per mol phosphorus, according to a hyperbolic relationship as shown ( $-88\text{ kJ/mol P}$  divided by  $r$ ).

All spectroscopic techniques used and the calorimetric study confirm that two different regimes can

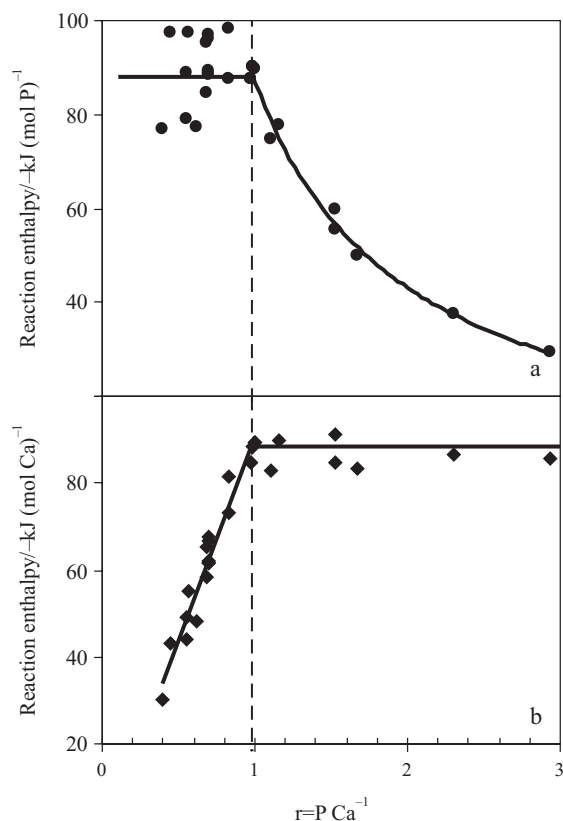
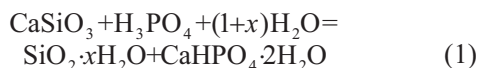


**Fig. 5** a – Reaction enthalpy/mol P and b – reaction enthalpy/mol Ca, obtained by the isothermal DSC experiments performed at 30°C as a function of  $r$ . The solid line for the a – reaction enthalpy/mol Ca is found by linear regression up to  $r=1$  and is the mean value for higher values of  $r$ . The solid line for the b – reaction enthalpy/mol P is the mean value up to  $r=1$  and follows the function  $y=88/r$  for higher values

be distinguished for the system wollastonite–phosphoric acid (13 mol% *ortho*-phosphoric acid) in the measured range. For molar ratios  $r$  between 0.39 and 1, only one type of calcium phosphate (brushite) is formed. The formation reaction of brushite ( $\text{CaHPO}_4 \cdot 2\text{H}_2\text{O}$ ) is represented in Eq. (1).



For  $r$  between 1 and 1.66 (highest measured value), three different calcium phosphates (brushite, monetite and calcium dihydrogenphosphate monohydrate) can be formed, depending on the molar ratio  $r$ . The reactions leading to monetite ( $\text{CaHPO}_4$ ) and calcium dihydrogenphosphate monohydrate ( $\text{Ca}(\text{H}_2\text{PO}_4)_2 \cdot \text{H}_2\text{O}$ ) are depicted in Eqs (2) and (3), respectively.

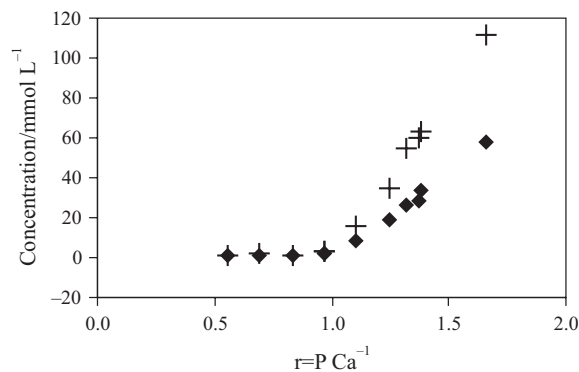
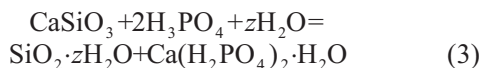
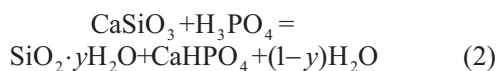


**Fig. 6** + – Soluble P and ♦ – Ca content after reaction as a function of  $r$

Note that brushite has a P/Ca ratio=1, thus the wollastonite can be reacted completely at  $r=1$  (Eq. (1)). For higher values of  $r$ , a component with P/Ca=2 is additionally formed (Eq. (3)) but its quantity is not sufficient to consume all of the phosphorous present. A substantial amount of soluble P and Ca is indeed retrieved after reaction for values of  $r$  above 1 as shown in Fig. 6. The formation of a compound with P/Ca=2 from  $r=1.4$  does not alter this increasing trend. Compositions in the range above  $r=1$  are for this reason not suited as a material.

## Conclusions

The model reaction of wollastonite particles suspended in a phosphoric acid solution (13 mol% *ortho*-phosphoric acid) leads to the formation of a cement-like material. The setting of the suspension, measured with DMA, starts at a conversion of about 33%. The reaction rate appears not to be influenced by the solidification and the reaction can be completed under isothermal conditions at 25°C. For mixtures with molar ratio phosphorus/calcium  $r$  up to 1, wollastonite is gradually transformed into brushite having a P/Ca ratio of one. If the molar ratio  $r$  is between 1 and 1.66, monetite and calcium dihydrogenphosphate monohydrate are also formed. Brushite seems to vanish at a ratio  $r$  of 1.4.  $^{31}\text{P}$  MAS NMR spectroscopy confirms that only monophosphates are present.  $^{29}\text{Si}$  MAS NMR and FTIR show that amorphous silica consisting of mainly  $\text{Q}^4$ ,  $\text{Q}^3$  and a minor amount of  $\text{Q}^2$  sites, is generated during the reaction. The main network modifier consists of protons.  $^1\text{H}$ -cross polarization  $^{29}\text{Si}$  MAS NMR spectra (having a very low signal to noise ratio) might indicate that these OH groups are involved in H-bridge exchange processes. For compositions with  $r>1$  a soluble fraction of P and Ca is observed.

## Acknowledgements

The authors wish to acknowledge M. P. Delplancke (Dept. Industrial Chemistry, ULB) for the XRD measurements. M. B. and R. W. are indebted to the Fund for Scientific Research – Flanders (Belgium) (FWO) (Grant G.0016.02) and to the Research Council of the VUB (Grants GOA31, OZR362, OZR875) for financial support. J. W. is indebted to the Research Council of the VUB (Grants GOA3 and OZR755).

## References

- 1 K. A. Milne, N. J. Calos, J. H. O'Donnell, C. H. L. Kennard, S. Vega and D. Marks, *J. Mater. Sci. – Mater. Med.*, 8 (1997) 349.
- 2 H. Chung-King, *Mater. Chem. Phys.*, 80 (2003) 409.
- 3 O. Pawlig and R. Trettin, *Thermochim. Acta*, 329 (1999) 7.
- 4 Y. Quanbing, Z. Beirong, Z. Shuqing and W. Xueli, *Cem. Concr. Res.*, 30 (2000) 1807.
- 5 J. Péra and J. Ambroise, *Cem. Concr. Compos.*, 20 (1998) 31.
- 6 L. C. Chow and S. Takagi, *J. Res. NIST*, 106 (2001) 1029.
- 7 W. D. Kingery, *J. Am. Ceram. Soc.*, 33 (1950) 239.
- 8 A. K. Chatterjee, Proceedings of the 9<sup>th</sup> International Congress on the Chemistry of Cement, New Delhi, India 1992, p. 177.
- 9 J. U. Otaigbe and G. H. Beall, *Trends Polym. Sci.*, 5 (1997) 369.
- 10 D. A. Hall, R. Stevens and B. El-Jazairi, *Cem. Concr. Res.*, 31 (2001) 455.
- 11 E. Soudée and J. Péra, *Cem. Concr. Res.*, 32 (2002) 153.
- 12 M. C. Connaway-Wagner, W. G. Klemperer and J. F. Young, *Chem. Mater.*, 3 (1991) 5.
- 13 G. Van Assche, A. Van Hemelrijck, H. Rahier and B. Van Mele, *Thermochim. Acta*, 286 (1996) 209.
- 14 H. Rahier, B. Van Mele and J. Wastiels, *J. Mater. Sci.*, 31 (1996) 80.
- 15 R. Laatikainen, M. Niemitz, W. J. Malaisse, M. Biesemans and R. Willem, *Magn. Reson. Med.*, 36 (1996) 359.
- 16 H. Rahier, J. F. De Nayer and B. Van Mele, *J. Mater. Sci.*, 38 (2003) 3131.
- 17 S. Swier, G. Van Assche, A. Van Hemelrijck, H. Rahier, E. Verdonck and B. Van Mele, *J. Thermal Anal.*, 54 (1998) 585.
- 18 G. Mosselmans, H. Rahier, M. Biesemans, M. Leermakers, B. Van Mele and J. Wastiels, to be submitted.
- 19 A. Tadayyon, S. M. Arifuzzaman and S. Rohani, *Ind. Eng. Chem. Res.*, 42 (2003) 6774.
- 20 G. Engelhardt and D. Michel, *High-Resolution Solid-State NMR of Silicates and Zeolites*, J. Wiley, Chichester 1987.
- 21 H. Rahier, W. Simons, M. Biesemans and B. Van Mele, *J. Mater. Sci.*, 32 (1997) 2237.
- 22 H. Rahier, B. Van Mele, M. Biesemans, X. Wu and J. Wastiels, *J. Mater. Sci.*, 31 (1996) 71.

---

DOI: 10.1007/s10973-006-8225-7